Tribology International 43 (2010) 277–282

Contents lists available at ScienceDirect

Tribology International

journal homepage: www.elsevier.com/locate/triboint

The role of fragility in EHL entrapment

Ashlie Martini [a,*], Scott Bair [b]

[a] Purdue University, School of Mechanical Engineering, 585 Purdue Mall, West Lafayette, IN 47907, USA
[b] Georgia Institute of Technology, Center for High-Pressure Rheology, George W. Woodruff School of Mechanical Engineering, Atlanta, GA, USA

ARTICLE INFO

Article history:
Received 13 April 2009
Received in revised form
2 June 2009
Accepted 3 June 2009
Available online 10 June 2009

Keywords:
Elastohydrodynamic lubrication
Lubricant rheology

ABSTRACT

Experimental measurements of time dependent film thickness in entrapped liquids, measurements of viscosity under pressure, and simulations using realistic pressure–viscosity models contribute to improved understanding of the mechanisms of entrapment formation and persistence. The ambient viscosity and pressure–viscosity coefficient affect entrapment only as much as they are predictors of behavior at much higher pressure. Fragile liquids, such as lubricating oils, experience rapid increase in sensitivity of dynamic properties to temperature and pressure as the glass transition is approached. The fragility property of lubricants appears to be of overwhelming importance to entrapment which experimental evidence indicates will reduce starting friction.

1. Introduction

There has been lately much interest in transient effects in elastohydrodynamic lubrication (EHL) and one of the most curious artifacts is the formation of a central axisymmetric dimple at the center of a circular contact, a liquid-filled entrapment, which may persist for hours after the motion of the bulk of the rollers has vanished. Entrapment may occur by a sudden halt to rolling/sliding motion [1,2] or by impact [3,4]. Entrapment may be more than merely a curiosity. The captured liquid is compressed to very high pressure and may support a significant portion of the contact load. The friction at the start-up of sliding should therefore be reduced when an entrapment is present if the force to shear the pressurized liquid is less than the force to shear the circular solid conjunction which it replaces.

To demonstrate the feasibility of entrapment eased start-up, in a preliminary experiment, friction was measured at the initiation of sliding with and without entrapment as illustrated in Fig. 1. Using the experimental arrangement described below, slow sliding was initiated after a gradual stop to prevent entrapment and also after a sudden stop which formed an entrapment. Both cases tend toward the same steady friction after 2 s, as expected. However, the entrapment apparently results in a lower residual shear force as shown by the data for negative time in Fig. 1 where the contact is stationary. The sliding friction is lower while the entrapment exists as shown by the plateau at 0.5–1.0 s where the friction coefficient is reduced from about 0.066–0.036. This effect can be repeated. After some sliding the entrapment is displaced to the edge whereupon the entrapped liquid drains away and the friction then returns to the entrapment free level after 1.5 s. The relatively slow time response of this friction measurement results from the large elastic compliance of the instrument which is designed for steady rolling traction measurements.

These results show that entrapment is not only an interesting phenomenon from a scientific standpoint, but may be a means of improving start-up efficiency. However, we cannot take full advantage of this utility until we understand which lubricant properties are active in entrapment formation and persistence. Towards this end, a transient EHL model-based study and qualitative experimental validation are presented with the goal of elucidating the lubricant properties that are important to entrapment. This particular analysis is unique in the use of a realistic description of the pressure-dependence of viscosity. Viscosity has not been adjusted to yield agreement with film thickness measurement. Instead, the viscosities of the experimental liquids have been measured in viscometers and fitted to pressure–viscosity models which are capable of describing pressure–fragility, a property of glass-forming liquids long ignored in EHL. Fragility is found to be a property of overwhelming importance to EHL entrapment.

2. Methodology

2.1. Experiment

Viscosities were measured in falling body viscometers which apply a shear stress sufficiently low (<100 Pa) so that the viscosities can be considered to be the limiting low shear values.

Two types of film thickness experiments were performed, sudden halting and impact. The quiescent loaded contact conditions were the same for either case: A sapphire disc is loaded against a steel ball of 7.6 mm radius with a force of 11.3 N by a weight suspended from the disc. The contact surface of the disc

* Corresponding author. Tel.: +1 765 494 6726.
E-mail address: a-martini@purdue.edu (A. Martini).

0301-679X/$ - see front matter © 2009 Elsevier Ltd. All rights reserved.
doi:10.1016/j.triboint.2009.06.006

Nomenclature

h	film thickness, m
h_c	central film thickness, m
K_0	isothermal bulk modulus at $p=0$, Pa
K'_0	pressure rate of change of isothermal bulk modulus at $p=0$
K_{00}	K_0 at zero absolute temperature, Pa
p	pressure, Pa
p_g	glass transition pressure, Pa
p_∞	pressure at which viscosity diverges, Pa
$p_{-\infty}$	tension at which the associated viscosity term vanishes, Pa
p_+, p_-	parameters in the Bair and Kottke pressure–viscosity model, Pa
r	radius, m
T	temperature, K
t	time, s
α	local pressure–viscosity coefficient, Pa^{-1}
α_0	conventional pressure–viscosity coefficient, Pa^{-1}
α^*	reciprocal asymptotic isoviscous pressure coefficient, Pa^{-1}
α_g	pressure–viscosity coefficient of the liquid at the glass transition, Pa^{-1}
α_n, α_p,	parameters of the Irving and Barlow model, Pa^{-1}
β_k	temperature coefficient of K_0, K^{-1}
μ	limiting low-shear and Newtonian viscosity, Pa s
μ_g	viscosity at the glass transition, Pa s
ρ	mass density, kg/m^3
ρ_0	mass density, at $p=0$, kg/m^3

has a semi-transparent metal coating to enhance optical interference so that the details of the film may be observed. The contact is illuminated with light filtered to have a narrow distribution of wavelength centered at 600 nm. The micrographs were calibrated with a stage micrometer. For film thickness measurement, the refractive index was assumed to be equal to 1.5 and the phase change on reflection was adjusted to yield a power-law relation between rolling velocity and film thickness.

Sliding motion results in the formation of a film about 300 nm thick. Slowly reducing the sliding speed to rest results in uniform contact. However, using a mechanical stop to rapidly bring the sliding to rest can result in a central entrapment. This method was applied to entrap a Mineral Oil and a Heavy polyalphaolefin (PAO). Entrapments can also be formed by normal motion of the surfaces. The disc with attached weight were lifted 1.8 mm above the ball and released in efforts to entrap a Light PAO and a polyol ester (POE).

2.2. Simulation

Entrapment formation was modeled using a full numerical transient solution for EHL point contact using only the Poiseuille and squeeze terms of the Reynolds equation which in spherical coordinates can be written as [5]

$$\frac{\partial}{\partial r}\left(\frac{\rho h^3}{\mu} r \frac{\partial p}{\partial r}\right) = 12r\frac{\partial(\rho h)}{\partial t} \qquad (1)$$

where h is film thickness, r is radial position, p is pressure, μ is viscosity, ρ is density, and t is time. The model includes elastic deformation of the solids as described by the Boussinesq approximation, load balance, the Tait pressure–density relationship, and multiple pressure–viscosity models described in the next section. The general solution approach is similar to that given in [6]. Some of the numerical methods described in [7] and references therein were employed for accurate and efficient solution of these equations. The computational domain is 0.22 mm square subdivided into 128 discrete units. The transient iteration scheme is solved using time steps of 0.716, 1.791, and 3.581 ms which were found to be small enough to capture even nanometer scale effects of lubricant properties on entrapment behavior. The larger step sizes were used only after (and if) the dynamics of the system slowed sufficiently to allow accurate numerical solution.

The Tait pressure–density model [8] was employed because it is known to be accurate both at moderate pressures and when extrapolated to very high pressures such as those required for

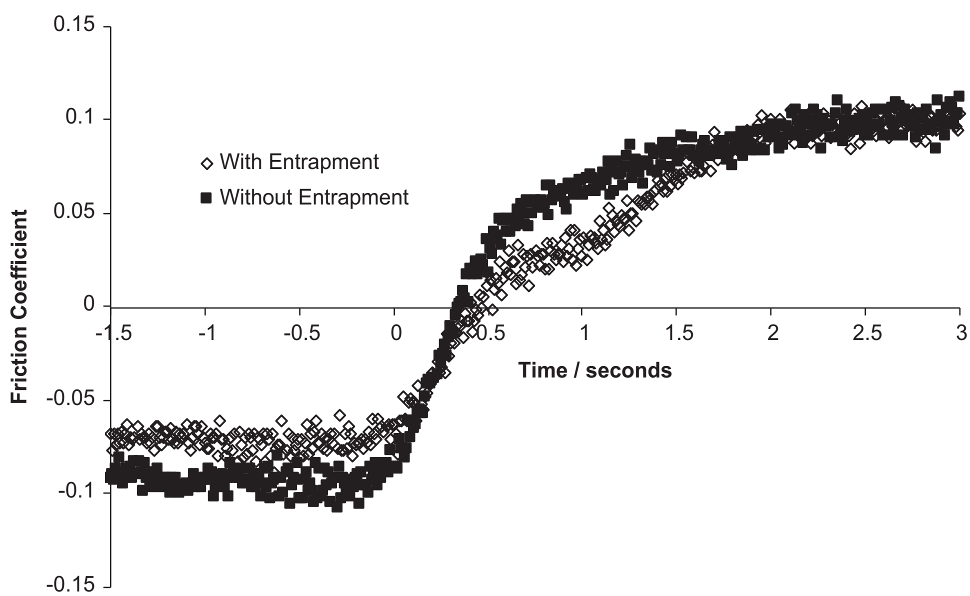

Fig. 1. Friction coefficient at start up with and without entrapment illustrating the potential utility of entrapment as a means of improving start up efficiency.